PHYSICAL REVIEW B **68**, 165321 (2003)

Atomic structure determination of the Si-rich β-SiC(001) 3×2 surface by grazing-incidence x-ray diffraction: A stress-driven reconstruction

M. D'angelo, H. Enriquez, V. Yu. Aristov,* and P. Soukiassian
Commissariat à l'Energie Atomique, Laboratoire Surfaces et Interfaces de Matériaux Avancés, Associé à l'Université de Paris-Sud/Orsay, DSM-DRECAM-SPCSI, Bâtiment 462, Saclay, 91191 Gif sur Yvette Cedex, France

G. Renaud, A. Barbier, and M. Noblet
Commissariat à l'Energie Atomique, DSM-DRFMC-SP2M, 85 X, 38041 Grenoble Cedex, France

S. Chiang
Department of Physics, University of California-Davis, Davis, California 95616-8677, USA

F. Semond
Centre National de la Recherche Scientifique, CRHEA, Sophia-Antipolis, 06650 Valbonne, France

(Received 22 April 2003; revised manuscript received 11 July 2003; published 16 October 2003)

The atomic structure of the Si-rich β-SiC(001) 3×2 surface reconstruction is solved by grazing-incidence x-ray diffraction with surface and subsurface structure determination. The reconstruction involves three Si atomic planes ($\frac{1}{3}+\frac{2}{3}+1$ Si monolayers) in qualitative agreement with *ab initio* theoretical calculations. The first plane includes Si dimers that are asymmetric with a 0.1 Å height difference between Si atoms while the second plane includes Si dimers having alternating long (2.41 Å) and short (2.26 Å) lengths resulting in long-range influence with no buckling of the top surface dimers, in strong contrast to other group-IV semiconductors. Dimerization is also shown to take place in the third Si plane with a dimer having a bond length at 2.38 Å. In addition, a large Si interlayer spacing is found between the reconstructed planes at 1.56 Å, significantly larger than that for bulk SiC (1.09 Å) and Si (1.35 Å) interlayer distances, indicating a very open surface. The results suggest that stress is at the origin of this complex surface organization.

DOI: 10.1103/PhysRevB.68.165321 PACS number(s): 68.35.Bs

I. INTRODUCTION

Silicon carbide (SiC) is a IV-IV wide-band-gap compound semiconductor that is of strong interest for advanced applications in ceramics, in nanotechnologies, and in micro- or optoelectronics devices and sensors. In addition, it is also an electronic material used in harsh environments because, e.g., of its excellent ability to resist to radiation damage.[1–5] Its figures of merit scale 2–3 orders of magnitude above all other semiconductors except diamond.[1–5] Furthermore, aside from its capability as an advanced semiconductor, SiC has interesting mechanical properties with a high hardness (the third hardest material after diamond and boron nitride) and is used in matrix composites.[6,7] Also, it is one of the best biocompatible materials.[8,9] Due to very close lattice parameters, SiC is a very promising substrate for the growth of III-V nitrides (which, unlike SiC, have a direct band gap), providing a large range of interesting applications in optoelectronics.[1–3] Because of the expected similarity to Si (Ge) in surface structure, the cubic β-SiC phase is of special interest.[4,5]

However, there are some very significant differences. Indeed, unlike elemental group-IV semiconductors such as Si, Ge or C, SiC is not a fully covalent semiconductor, with a significant charge transfer between Si and C resulting in the formation of polar surfaces.[10,11]

In addition, surface stress plays a central role in SiC surface ordering due to large mismatches in lattice parameters (20% smaller than that for Si and 22% larger than that for diamond).[5] This suggests that Si atoms located at the β-SiC surface could be compressed by 20% when compared to a corresponding silicon surface. While β-SiC has a smaller band gap than hexagonal $4H$- or $6H$-SiC polytypes (2.4 eV instead of 3.3 or 2.9 eV, respectively), the carrier mobilities are much higher for the cubic polytype, which also has an average factor of merit scaling nearly 1 order of magnitude above those of hexagonal SiC.[1–3] The latter is primarily preferred for high-power electronic devices.[1–3] Instead, β-SiC is especially suitable for high-frequency devices particularly important in communications systems such as power base stations for mobile phones. The accurate knowledge of the SiC surface structure is of both fundamental and applied importance in a large variety of problems such as metal/SiC or insulator/SiC interface formation. Atomic control of β-SiC(001) surfaces has been achieved only recently showing the existence, depending on surface stoichiometry, of many reconstructions such as Si-rich 3×2, 8×2, 5×2, $7\times2,\ldots,(2n+1)\times2$, Si-terminated $c(4\times2)$, C-terminated $c(2\times2)$, and C-rich graphitic 1×1.[5]

In this context, the Si-rich surface is of special interest because its 3×2 reconstruction includes, depending on the model considered, one or two additional Si atomic planes on top of a Si-terminated β-SiC(001) stressed surface with nothing equivalent for corresponding Si or Ge surfaces.[10,11] Of strong technological importance, such Si-rich SiC surfaces are known to be much more reactive to hydrogen and to oxygen (by about 3 orders of magnitude) when compared to silicon, with initial oxygen/hydrogen insertion occurring well below the surface.[12–15] However, the β-SiC(001) 3×2 surface and subsurface structures are still under debate. Many different opposite models have been proposed based on structural and nonstructural experimental techniques such as low-energy electron diffraction (LEED), reflection high-energy electron diffraction (RHEED), medium-energy ion scattering (MEIS), real-space atom-resolved scanning tunneling microscopy (STM), Auger and photoemission spectroscopies,[16–24] and also a few *ab initio* total-energy theoretical calculations.[25–27] These include (i) the double dimer row model (DDRM) with a surface terminated by a $\frac{2}{3}$ monolayer (ML) Si,[16,12,20,22–24] (ii) the single dimer row model (SDRM) terminated by a $\frac{1}{3}$-ML Si,[19] (iii) the alternate dimer row model (ADRM) predicted theoretically and having 2 ×3 reconstruction with a $\frac{1}{3}$ Si ML coverage and asymmetric dimers,[25,26] (iv) another ADRM having a 3×2 surface array and asymmetric dimers as established by atom-resolved scanning tunneling microscopy (STM),[21] and finally, (v) a two adlayer asymmetric dimer model (TAADM) predicted by *ab initio* pseudopotential total-energy and grand canonical potential calculations.[27] The TAADM is basically the ADRM 3×2 model built on top of the DDRM. The schematic of these different models are shown in Fig. 1.

Real-space STM measurements performed into both filled and empty electronic states[21] has brought very significant insights on the topmost surface structure. When tunneling into the empty electronic states, the two atoms forming the Si-Si dimer could be resolved, allowing a clear identification of the dimer position and direction.[21] The surface was shown to organize in rows of asymmetric dimers perpendicular to the rows and all tilted in the same direction. These measurements clearly indicate that both DDRM (Refs. 16, 12, 20 and 22–24) and SDRM (Ref. 19) cannot account for the surface structure. However, with the STM measurements, being sensitive to the topmost atomic layer only, it was not possible to draw a complete picture of the surface structure from these experiments only, with no structural information about the subsurface region. In particular, the ADRM does not determine how the Si-Si dimers of the adlayer may be connected to the underlying Si plane since the latter can undergo 2 ×1 reconstruction. In this view, the TAADM derived from theoretical calculations[27] has to be considered. The TAADM was apparently supported by other calculations of the reflectance anisotropy spectroscopy (RAS).[28] The calculated spectrum was claimed to be in agreement with available data from experimental reflectance difference spectroscopy (RDS).[29] However, the calculated RAS spectrum[28] for the DDRM (Refs. 16, 12, 20, and 22–24) is also close to the experimental spectrum with two similar broad spectral features located at the same energy.[29] In addition, the experimental $\Delta R/R=2(R_{[1\bar{1}0]}-R_{[110]})/(R_{[110]}+R_{[1\bar{1}0]})$ (Ref. 29) spectrum is not correctly reported in Ref. 28 with the opposite sign as $2(R_{[110]}-R_{[1\bar{1}0]})/(R_{[110]}+R_{[1\bar{1}0]})$, making a comparison with theory difficult. Also, the electronic band structure[27] calculated for the TAADM was claimed to be in best agreement with the experimental band structure[22,23] when compared to those calculated for the DDRM and SDRM.[27] But this agreement is good for some part of the two-dimensional (2D) Brillouin zone for two flat bands only, with no experimental data available between the J-M and the M-J' direction.[22,23,27] In this respect, the agreement for the SDRM could also be found reasonable, with a 0.3-eV discrepancy for one of the bands only (along Γ-J), within the calculation accuracy limits.[27] Thus, no real insight could be drawn from these optical or electronic properties studies.[27–29]

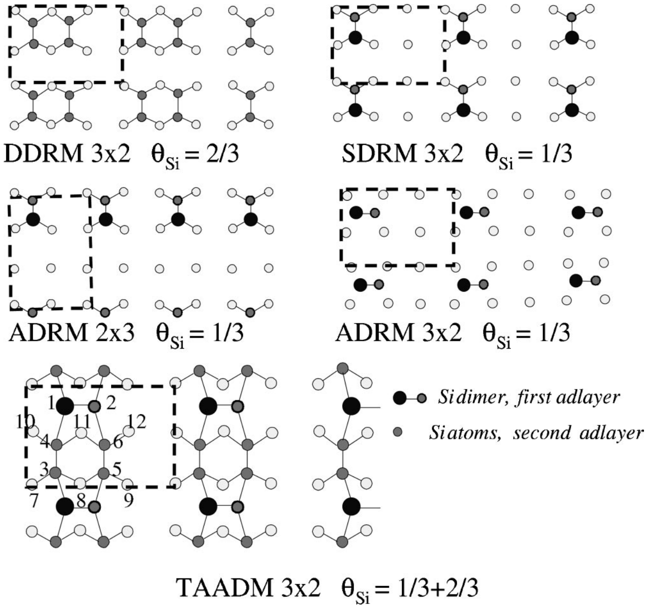

FIG. 1. Schematic top views of the β-SiC(001) 3×2 surface reconstruction proposed models: (a) DDRM (Refs. 16, 17, and 20), (b) SDRM (Ref. 19), (c) ADRM 2×3 (Refs. 25 and 26), (d) ADRM 3×2 (Ref. 21), and (e) TAADM (Ref. 20). The corresponding primitive 3×2 (2×3) surface unit cell is indicated by a dashed line.

In this article, we use synchrotron-radiation-based grazing-incidence x-ray diffraction (GIXRD) to determine the β-SiC(001) 3×2 surface structure. The latter is found to be in qualitative agreement with the theoretical TAADM. Our results provide important details on the subsurface structure. The surface reconstruction includes three Si atomic planes separated by interlayer distances much larger than in bulk SiC or Si. The second plane has alternating long (2.41-Å) and short (2.26-Å) Si dimers (ALSD's) that minimize the surface stress. Such an array has a long-range influence that explains the lack of dimer anticorrelation in the topmost atomic layer, in strong contrast to silicon or germanium.

II. EXPERIMENTAL DETAILS

The GIXRD experiments are performed on the CRG-IF (BM32) beamline at the European Synchrotron Radiation Facility (ESRF, Grenoble) at a pressure of 3×10^{-11} Torr during the data acquisition, maintaining a very high surface quality during all measurements. In the recent years, GIXRD using synchrotron radiation has been especially successful in solving accurately complex surface structures when the underlying crystal is of high structural quality.[30–32] So far, there is no GIXRD study available for the β-SiC surface. Because of the lack of high-quality β-SiC single crystals, such an experiment has to be performed on thin films (1 μm). However, the latter are grown by chemical vapor deposition (CVD) on a carbonized Si(100) wafer with a buffer layer at the SiC/Si interface having rather large stacking-fault defect densities, making surface measurements especially challenging. In order to eliminate the contribution coming from the stacking faults located in the buffer layer at the SiC/Si interface, we use a low photon energy at 12 keV, with the incident angle being kept at the critical value (0.176°). As compared to a standard semiconductor study, the probed reciprocal space area is therefore limited. In addition, a specific sample mounting is needed for homogeneous high-temperature annealings through direct current heating, limiting even more the reciprocal-space exploration.

High-quality β-SiC(001) 3×2 single domain surfaces are checked by RHEED and GIXRD. The basis vectors ($\mathbf{a}_S, \mathbf{b}_S, \mathbf{c}_S$) of the surface reconstruction unit cell are related to the bulk ones by $\mathbf{a}_S \| [110]_{\mathrm{bulk}}$, $\mathbf{b}_S \| [1\bar{1}0]_{\mathrm{bulk}}$, $\mathbf{c}_S \| [001]_{\mathrm{bulk}}$, with $a_S = b_S = 3.088$ Å and $c_S = 4.367$ Å. The reciprocal space is described by its reduced coordinates (*h,k,l*), *l* being perpendicular to the surface. Two complete sets of data (measured from two distinct 3×2 surfaces) are in excellent agreement. For each set, we measure 78 in-plane (excluding integer-order) and 276 out-of plane reflections, along eight rods, and 168 reflections along five crystal truncation rods (CTR's).[30–32] Additional details about high-quality preparation of the β-SiC(001) 3×2 surface reconstruction and GIXRD experiments and data analysis can be found elsewhere.[5,21,30–32]

III. RESULTS

We first look at the in-plane diffracted intensity map measured for the surface at $l=0.05$ and at the corresponding experimental Patterson contour over the 3×2 unit cell (Fig. 2). The measured $\times2$ diffracted spots are not represented because they have intensities more than 10 times weaker than the $\times1$ ones, making any comparison with the calculated intensities difficult. This much weaker intensity is correlated to the existence of dimer-pair *B* defects as identified by STM.[21] These *B* defects are at the origin of long antiphase boundaries spreading the intensity of the $\times2$ reflections in reciprocal space, thus strongly weakening the $\times2$ intensity (as also observed by LEED and RHEED) and leaving the $\times1$ intensity dominant.[5,16,17] The in-plane diffraction diagram exhibits a $p2mm$ symmetry, indicating either a $p2mm$ or a $p1m$ or a $pm1$ surface symmetry. We will see below that the rod profiles look symmetric within the experimental error bars and therefore bring no further information to conclude about the symmetry. Notice that the DDRM would correspond to a $p2mm$ symmetry, whereas SDRM, ADRM, and TAADM correspond to a $p2mm$ symmetry only if the dimers are symmetric and to a $p1m$ symmetry for asymmetric dimers. The experimental Patterson function (Fig. 2) clearly indicates that along the [110] direction, the dominant interatomic distance is a multiple of $\frac{1}{5}$ of the reconstructed unit cell. From this observation, we deduce that, along the [110] direction, the atoms in the last Si plane cannot be regularly spaced by one-third of the reconstructed unit-cell length, deviating from the bulk positions.

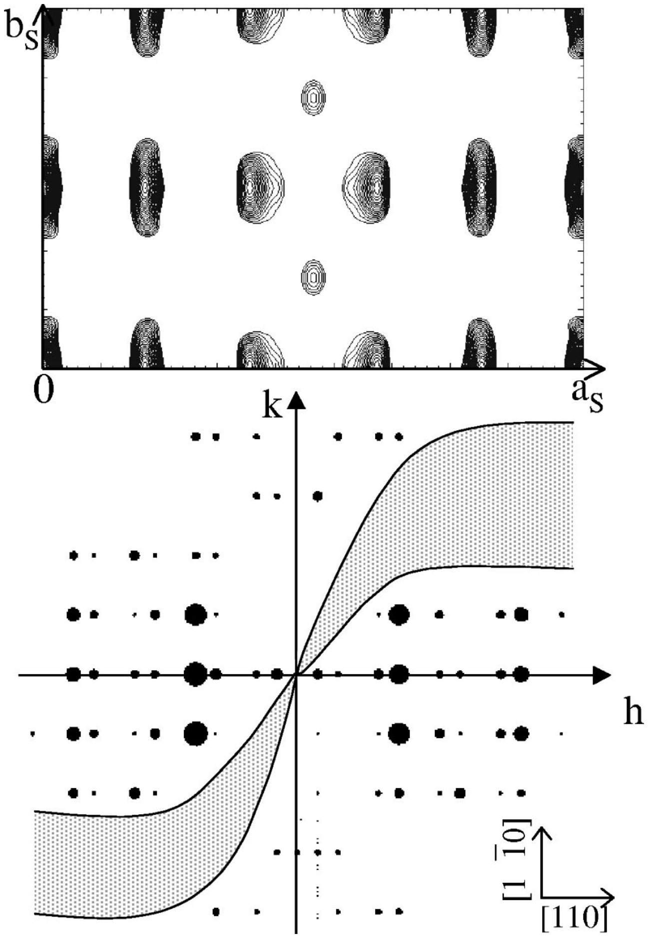

FIG. 2. (a) Experimental Patterson contour plot for the β-SiC(001) 3×2 surface for the TAADM, represented over the whole 3×2 unit cell. 100 contour levels are used between the 0.14 and 1 minimal and maximal values. (b) In-plane diffracted intensity map for the β-SiC(001) 3×2 surface measured at $l=0.05$. The radii are proportional to the structure factor modulus. The measured $\times2$ diffracted spots are not represented. The *h* and *k* indices are related to the 3×2 reconstructed unit cell. The shaded area corresponds, in the reciprocal space, to the part of the surface hidden by the sample electrical contacts, which may hide the grazing-incidence beam as well as the scattered beam.

We proceed to a preliminary fitting procedure, assuming that the adlayer dimers are symmetric, and hence a $p2mm$ symmetry with two mirrors in the unit cell. In order to roughly discriminate between the different 3×2 models, we first fit the in-plane data only, including 28 inequivalent reflections for a $p2mm$ symmetry averaging with a systematic uncertainty of 9.5%. The fitting procedure includes the minimum fitting parameters necessary to leave the atomic positions move, in agreement with the two mirror-symmetry conditions. Only one parameter is required to make the atomic positions relax along the [110] direction. Depending on the model, one, two, or three additional parameters are required

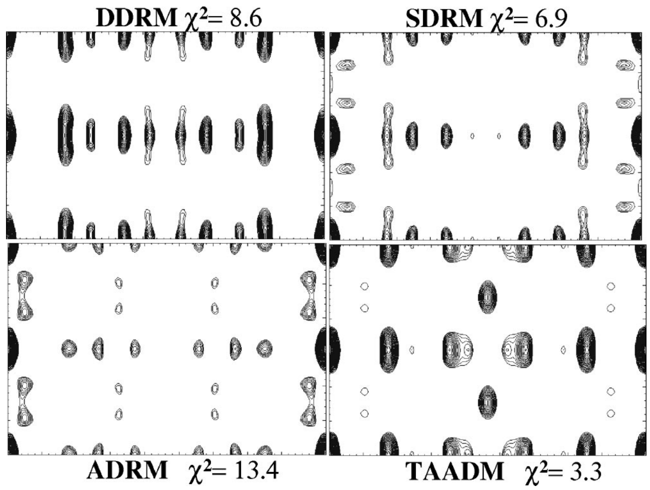

FIG. 3. Patterson contour plots calculated for the different models DDRM, SDRM, ADRM, TAADM. The atomic positions are derived from the in-plane diffracted intensity fitting procedure, in the frame of a $p2mm$ symmetry. Both the dimer lengths and the spacing between dimers in the unit cell are relaxed. The corresponding χ^2 agreement factor is indicated for each model.

to relax the length of the dimers and the spacing between dimers in the unit cell. The final χ^2 fitting agreement factors for the four proposed models for the 3×2 are 13.4 (ADRM), 8.6 (DDRM), 6.9 (SDRM), and 3.3 (TAADM). The first three values are very far away from the ideal $\chi^2=1$ value. Moreover, the corresponding calculated Patterson functions (Fig. 3) strongly differ from the experimental functions. Only the TAADM yields an acceptable agreement factor at this stage, with a Patterson map similar to the experimental map. Adding another fitting parameter (bringing the total to five independent parameters) to relax the atoms of the last atomic plane along the $[1\bar{1}0]$ direction improves the agreement factor to $\chi^2=2.5$.

Therefore, this preliminary analysis shows that a surface structure as complex as that proposed in the TAADM including one full Si atomic plane and two adlayers—is necessary to account for experimental in-plane diffraction data. We have now to refine the atomic positions involved in the surface reconstruction. Relaxing both in-plane and out-of-plane atomic positions leads to a $\chi^2=1.47$ agreement factor with eight independent parameters for the whole reconstruction rods intensities (29 in-plane and 157 out-of-plane inequivalent reflections for a $p2mm$ symmetry).

As suggested by the STM observation of asymmetric dimers, we next explore a surface of $p1m$ symmetry and consider the whole (noninteger) in-plane and out-of-plane reconstruction rod diffraction intensities, including, respectively, 35 and 240 inequivalent reflections after $p1m$ symmetry averaging. Many fitting parameters can be considered in the frame of a $p1m$ symmetry. The 12 Si atoms involved in one unit cell are numbered from 1 to 12 as depicted in Fig. 1. In the frame of $p1m$ symmetry, atoms Si_1 and Si_2 may not be equivalent, also dimers Si_3-Si_4 and Si_5-Si_6, as well as Si_7 and Si_9, and Si_{10} and Si_{12} atoms located in the last atomic plane. In order to choose only the minimum pertinent fitting parameters, we test different fitting procedures. Our criteria involve the value of the χ^2 agreement factor, as well as the pertinence of the atomic positions obtained. Since the in-plane data are much less "noisy" (averaging a 15% statistical error of the structure factor amplitude) than the out-of-plane reconstruction rods (25% statistical error), we systematically check if the in-plane data considered separately are in good agreement with the fitting procedure results.

Table I summarizes the results of the different fitting procedures. For a satisfactory fitting, an asymmetry of the top Si_1-Si_2 dimer must be considered, as well as an asymmetry between the underlying Si_3-Si_4 and Si_5-Si_6 dimer lengths. We also check that the introduction of any other asymmetry is not relevant. The fitting procedure involves 12 fitting parameters, including 7 in-plane and 4 out-of-plane fitting parameters, plus an overall scale factor. Notice that the error bars derived from the refinement program are uncorrelated. The Debye-Waller temperature factors have been set at the bulk value for all atoms, because no improvement could be achieved when fitting this parameter. For the whole data set (in-plane and out-of-plane), the agreement factor is $\chi^2=1.2$

TABLE I. Comparison between different fitting procedures with $p1m$ symmetry. For each procedure, we report (i) in the first column the assumptions relative to the relaxations of the atomic positions, (ii) in the second column the agreement factor for the fit of the whole data set (including in-plane and out-of-plane reflections), and (iii) in the third column, the agreement factor of the (ii) fit results for the in-plane data considered separately.

Fitting of the whole in-plane and out-of-plane reflections assuming:	Fitting χ^2 agreement factor	χ^2 agreement factor to the in-plane reflections only
Asymmetric 1-2 dimer	1.6	5.5
Symmetric 1-2 dimer and asymmetric 3-4/5-6 dimers lengths	1.33	4
Asymmetric 1-2 dimer and asymmetric 3-4/5-6 dimer positions	1.6	4.5
Asymmetric 1-2 dimer and asymmetric 3-4/5-6 dimers lengths	1.2	2

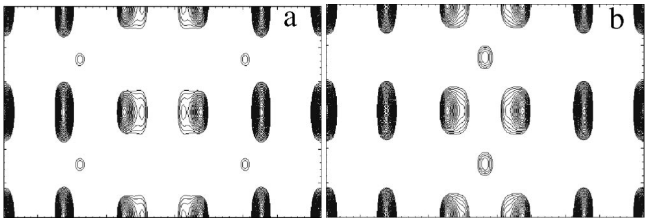

FIG. 4. Calculated Patterson contour plots for the β-SiC(001) 3×2 surface for a $p1m$ symmetry, represented over the whole 3×2 unit cell. 100 contour levels are used between the 0.14 and 1 minimal and maximal values. (a) The atomic positions considered are derived from the fit of in-plane and out-of-plane reconstruction rod diffraction intensities, with a $\chi^2=1.2$ agreement factor (cf. Table I). (b) The atomic positions considered are derived from the fit of in-plane diffraction intensities only, with a $\chi^2=1.3$ agreement factor.

and the residual $R=0.19$, which has to be compared to the $\chi^2=1.47$ agreement factor and $R=0.19$ residual obtained when assuming a $p2mm$ symmetry. Using the atomic positions derived from this fit leads to a satisfactory $\chi^2=2$ agreement factor for the 35 inequivalent in-plane diffraction intensities. The comparison between the experimental and calculated Patterson functions is shown in Fig. 4(a).

We now turn to the main features derived from this fit. First, a 1.56±0.04 Å interlayer spacing is found between the three planes involved in the reconstruction. This value is much larger than the SiC bulk interlayer spacing (1.09 Å) and even larger than the silicon bulk interlayer spacing (1.36 Å). In the last Si atomic plane located just above the first C plane, two Si dimers are formed, Si_9-Si_7 and Si_{12}-Si_{10}, having bond lengths of 2.38±0.02 Å, in good agreement with the calculated theoretical value of 2.41 Å.[27] Subsequently, the interatomic distance between atoms 7 and 8, 8 and 9, 10 and 11, and 11 and 12 is 3.43±0.01 Å instead of 3.08 Å for the bulk value and, in the second adlayer, Si_3-Si_4 and Si_5-Si_6 dimers are found to be distant by 3.48±0.01 Å. Finally, the topmost Si_1-Si_2 dimer is found to be asymmetric with the up atom located 0.1±0.05 Å higher than the down one, at a much lower value than the calculated theoretical one (0.5 Å).[20] Moreover, we find for this Si_1-Si_2 dimer a bond length at 2.78±0.03 Å, significantly larger than the theoretical value of 2.24 Å.[27] Table II provides the reduced (*X,Y,Z*) coordinates of the 12 Si atoms involved in the 3×2 reconstruction cell.

Most interestingly, in the second plane, we find that the underlying dimers do not have the same bond lengths with alternating long D_L (2.41±0.08 Å) and short D_S (2.26±0.08 Å) dimers. The long D_L and short D_S dimers are bonded on both sides to the A_U and A_D atoms belonging to the topmost asymmetric dimer. However, the agreement factor sensitivity indicates a rather large error bar (0.08 Å) to be compared to the 0.15-Å length difference found between D_L and D_S dimers. This uncertainty is induced by the lack of ×2 diffracted spots in our experimental data set along the dimer direction, and by the experimental error bars. As a comparison, we can also proceed to the partial fit of the in-plane data for which the experimental error bars are smaller. Although no complete model can be derived from such a procedure, the occurrence of short and long dimers is further confirmed, with even a higher length difference at 0.23±0.05 Å, a $\chi^2=1.3$ agreement factor and a calculated Patterson function in better agreement with the experimental one [Fig. 4(b)]. We can also note that this fit of the in-plane data leads to a smaller value at 2.5 Å for the Si_1-Si_2 dimer length, however, still far away from the calculated theoretical value of 2.24 Å.[27]

Figure 5 gives a set of representative intensity profiles along the (50*l*), (52*l*), (10*l*) and (80*l*) reconstruction rods. The fitting curve derived from the previous fit exhibits a modulation period varying from 2.5 to 2.8 in reciprocal-lattice units, which corresponds to a direct space thickness of 1.7 Å. With a 1.56 Å interlayer spacing, this clearly indicates that more than 2 atomic planes are involved in the reconstruction. The profiles of the (30*l*) and (60*l*) CTR's are in qualitative agreement with the fitting curves.

To determine the registry of the reconstruction with respect to the bulk, the CTR diffraction intensities are fitted-

TABLE II. Reduced (*X,Y,Z*) coordinates of the 12 Si atoms involved in the 3×2 reconstruction cell.

Si atom number	*X* (in-plane, along the ×3 direction)	*Y* (in-plane, along the ×2 direction)	*Z* (out-of-plane)
1	0.240±0.002	0	0.72±0.007
2	0.542±0.002	0	0.70±0.007
3	0.182±0.001	0.3045±0.0037	0.357±0.004
4	0.182±0.001	0.6955±0.0037	0.357±0.004
5	0.560±0.001	0.3166±0.0037	0.357±0.004
6	0.560±0.001	0.6834±0.0037	0.357±0.004
7	0.0000±0.001	−0.225±0.001	0±0.006
8	0.371	−0.225	0±0.006
9	0.742±0.001	−0.225±0.001	0±0.006
10	0.0000±0.001	0.225±0.001	0±0.006
11	0.37100	0.225	0±0.006
12	0.7420±0.001	0.225±0.001	0±0.006

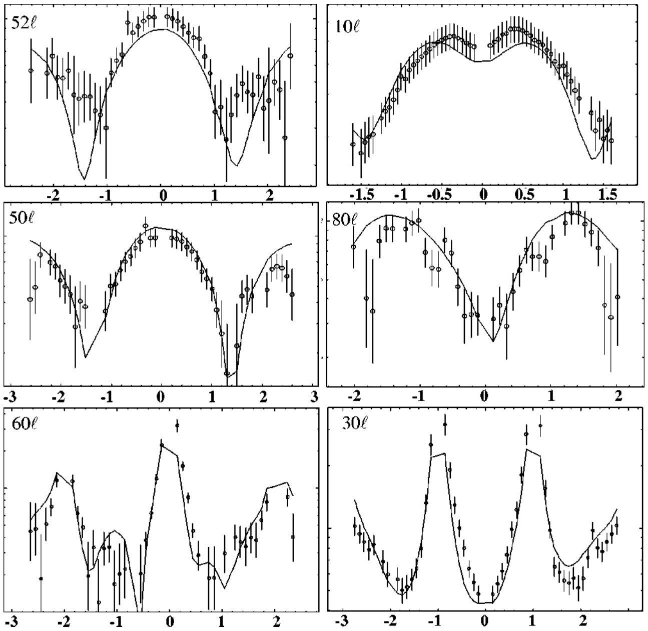

FIG. 5. $(5\overline{2}l)$, $(10l)$, $(50l)$, and $(80l)$ reconstruction rods and $(60l)$ and $(30l)$ CTR profiles with the error bars and corresponding fits. The logarithm of the absolute value of the structure factor is represented as a function of the out-of-plane reciprocal-lattice coordinate *l*.

with two shift parameters in agreement with a $p1m$ symmetry, along the [001] and the [110] directions, while the atomic positions within the reconstruction unit cell are kept fixed. With a $\chi^2=2.5$ agreement factor, the fit of the 149 inequivalent reflections indicates a negligible surface roughness [note that an average terrace length of 300 Å was deduced from the width of the (300) anti-Bragg reflection, in excellent agreement with the STM measurements[21]]. Along the [001] direction, the interlayer distance between the third Si atomic plane and the underlying C atomic plane deviates very slightly (0.03 Å difference) from the bulk interlayer distance. This slight deviation of the atomic positions in the third plane from the bulk positions along the z axis is in agreement with the previous reconstruction rod fit. Along the $[1\overline{1}0]$ direction, the C atoms of the underlying atomic plane show no shift with respect to the Si atoms 8 and 11.

The profiles of the $(30l)$ and $(60l)$ CTR are in qualitative agreement with the fitting curves. However, the agreement is not excellent, accordingly with the $\chi^2=2.5$ factor obtained on the CTR's alone. For the whole data set, including reconstruction rod and CTR data, the agreement factor is $\chi^2=1.78$ and the residual $R=0.23$. No significant improvement can be achieved when trying to fit again the reconstruction atomic positions to the data set including the CTR data.

Figure 6 displays the schematic model of the surface, with top and side views of the β-SiC(001) 3×2 reconstruction. It shows that the 3×2 reconstruction extends along three atomic planes distant by about $a_0/3$ (a_0 being the lattice parameter) instead of $a_0/4$ in the bulk, which emphasizes the very open character of this particular surface. The CTR fit shows that the bulk interlayer spacing of $a_0/4$ is recovered between the last Si atomic plane and the underlying first C atomic plane. For the topmost Si plane the Si A_U-A_D dimer is found to have a bond length of 2.78 ± 0.03 Å and is asymmetric with the A_U up atom being 0.1 ± 0.05 Å higher than the A_D down one. This value can be compared to the 0.2-Å height difference between up and down dimers in the Si-terminated β-SiC(001) $c(4\times2)$ surface reconstruction.[33] Most interestingly, the underlying dimers (belonging to the second plane) do not have the same bond lengths with alternating long D_L (2.41 Å) and short D_S (2.26 Å) dimers. The long D_L and short D_S dimers are bonded on both sides to the A_U and A_D atoms belonging to the top asymmetric dimer.[21] In the third atomic plane two 2.38-Å Si-Si dimers are formed per unit cell, so that the distance between the Si atoms bonded to the long D_L and short D_S dimers is equal to 3.43 Å, i.e., 11% larger than the 3.08-Å unit-cell parameter. Therefore the reconstructed structure involving three atomic planes is expanded both in-plane by 11% and out-of-plane by about 30%.

IV. DISCUSSION

The above GIXRD results support a model of the Si-rich β-SiC(001) 3×2 surface reconstruction involving three Si atomic planes ($\frac{1}{3}+\frac{2}{3}+1$ ML Si). They clearly rule out the DDRM, SDRM, and ADRM[16–26] for which no reasonable fitting could be found. They are in good qualitative agreement with the theoretical TAADM[27] for which a successful fitting procedure including the minimum number of parameters could be achieved. However, our measurements bring significant insights into the knowledge and understanding of the 3×2 surface structure. They are in excellent agreement with the presence of asymmetric dimers perpendicular to the dimer rows, all tilted in the same direction, as previously evidenced by real space atom-resolved empty electronic states STM imaging which, once again, cannot provide insight into the sub-surface region.[21]

The GIXRD results show also some significant differences from the theoretical TAADM. First, we find a smaller height difference between the up and down atoms of the top dimer at 0.1 Å (instead of 0.5 Å for the calculated value[27]). The length of this topmost dimer is rather large with values at 2.78 Å (if one considers the fit of the in-plane and out-of-plane diffraction intensities) or 2.5 Å (when considering the in-plane intensities only), instead of 2.24 Å for the calculated value.[27] Notice that the out-of-plane data are affected by a rather low signal-to-noise ratio, which suggests that the real value for the top Si-Si dimer bond length is lying between 2.78 and 2.5 Å. Most interestingly, we find that the second Si atomic layer ($\theta_{\mathrm{Si}}=\frac{2}{3}$) includes dimer rows having ALSD's with lengths of 2.41 ± 0.08 Å and 2.26 ± 0.08 Å. Indeed, one should remember that this second Si layer is lying on a 1-ML Si atomic stressed plane.[27,33,34] Without being covered by an excess of Si atoms as in the 3×2 surface reconstruction, this 1-ML atomic plane would form a Si-terminated β-SiC(001) $c(4\times2)$ surface reconstruction with alternately up and down dimers (AUDD's), reducing the surface stress.[33] One can therefore easily imagine that, when this surface is covered by additional Si layers, the AUDD arrangement cannot take

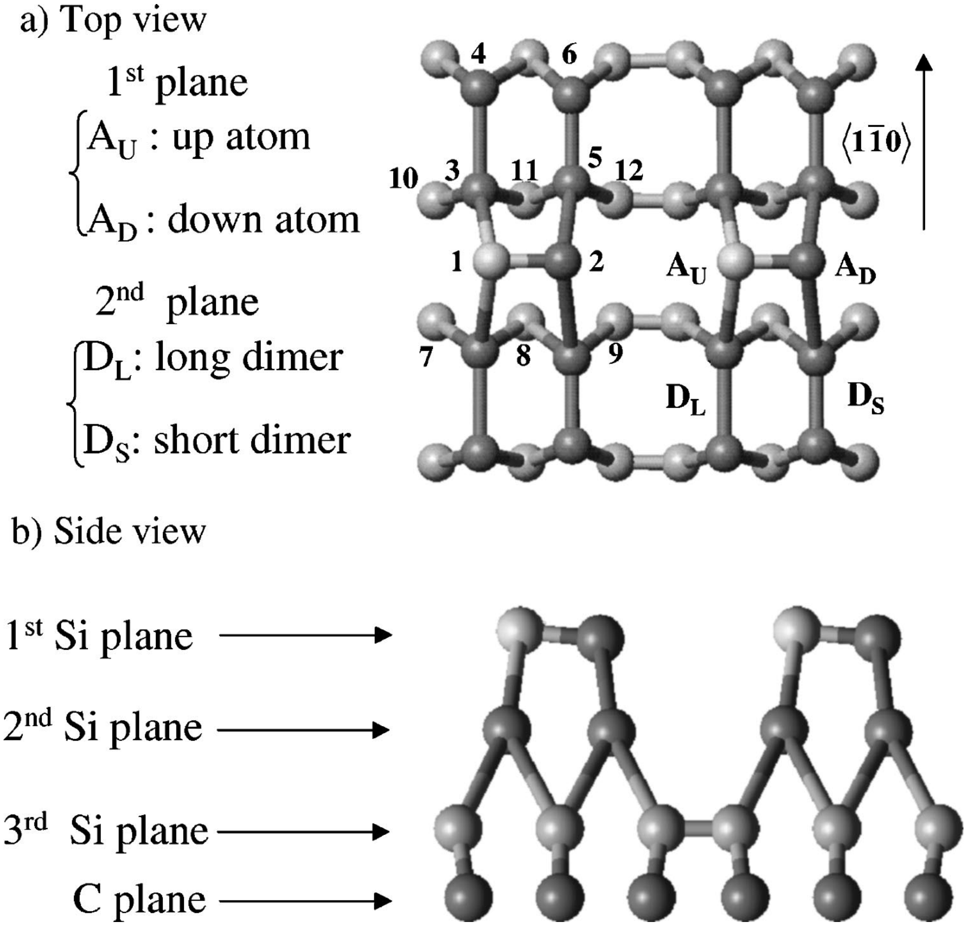

FIG. 6. (a) Top and (b) side views of the β-SiC(001) 3×2 surface reconstruction showing the three Si atomic planes with the top A_U-A_D asymmetric dimers (first plane) and the ALSD's having alternating long D_L and short D_S lengths in the second plane. In the side view, the underlying C plane of the bulk structure is also represented.

place leading to stress transfer to the upper Si layer. Our GIXRD results precisely indicate that in the 1-ML Si layer, the atoms deviate only slightly from bulk positions. A possible arrangement for the $\frac{2}{3}$-ML Si subsurface layer would consist of dimers with alternating heights [like the AUDD's for the $c(4\times2)$]. This cannot take place, however, because this subsurface Si layer is itself also covered by an additional $\frac{1}{3}$-ML Si. Therefore, another way to relax the stress and minimize the energy in this intermediate layer would be to have dimers having alternating long and short lengths precisely as found here (Fig. 6). In turn, this would affect the above A_U-A_D dimer, the long D_L dimer tending to push up the A_U atom while the short D_S dimer would instead tend to pull down the A_D atom, leading to the formation of an asymmetric dimer, as initially evidenced by real-space atom-resolved STM,[21] later by theoretical calculations,[27] and now by our GIXRD measurements. Most interestingly, this has a long-range influence explaining why the asymmetric A_U-A_D dimers forming the 3×2 surface reconstruction are all tilted along the same direction (not anticorrelated[15]) with no buckling, in strong contrast to the corresponding Si(001) or Ge(001) $c(4\times2)$ surface reconstructions.[10,11]

Most interestingly, the above ALSD model indicates a very open β-SiC(001) 3×2 surface reconstruction having a large distance between the first and second and between the second and third Si atomic planes at 1.56 Å, significantly larger than the interatomic layer spacing in bulk SiC and bulk Si with values at 1.09 and 1.35 Å, respectively. Furthermore, a 3.43-Å distance between nondimerized Si atoms within the same third plane is also significantly larger than the bulk value at 3.08 Å. It is interesting to correlate this finding with the rather high reactivity of the Si-rich β-SiC(001) 3×2 surface with simple adsorbates such as hydrogen or oxygen when compared to silicon, with H or O atom insertion into the subsurface region taking place already at very low exposures.[12,15] This indicates that this very open surface facilitates hydrogen or oxygen atom insertion into the β-SiC(001) lattice, which is of both strong fundamental interest and technological importance.

V. CONCLUSIONS

In conclusion, the atomic structure of the Si-rich β-SiC(001) 3×2 surface reconstruction has been determined by GIXRD. DDRM, SDRM, and ADRM are ruled out. The results are in qualitative agreement with the theoretically predicted TAADM, which gives a good description of the surface morphology. However, there are significant differences concerning the atomic positions and the bond lengths. The reconstruction involves three Si atomic planes having Si coverages of $\frac{1}{3}$, $\frac{2}{3}$, and 1 ML from top to bottom. A large interlayer spacing between the Si reconstructed planes is found with a separation of 1.56 Å between planes, significantly larger than that for the bulk-SiC (1.09 Å) and the bulk Si (1.35 Å) interlayer distances, indicating a very open β-SiC(001) 3×2 surface. Most significantly, a subsurface layer having alternating long (2.41 Å) and short (2.26 Å) dimers is found. This ALSD model is further supported by recent photoelectron diffraction measurements performed at the Advanced Light Source (ALS, Berkeley).[35] Such an ALSD array tends to minimize the strain and significantly influences the surface organization, leading to the top atomic plane dimers all being tilted in the same direction. This situation is in strong contrast to the behavior of elemental group-IV semiconductor surfaces in which dimer buckling is occurring. Dimerization is also taking place in the third Si plane with a dimer bond length at 2.38 Å. This study clarifies the β-SiC(001) 3×2 surface atomic structure, which has been under investigation for more than a decade. It also brings significant quantitative insight into stress-driven surface and subsurface atomic organization that can lead to rather complex structures.

ACKNOWLEDGMENTS

We are grateful to the European Synchrotron Radiation Facility ESRF (Grenoble) staff for expert and outstanding technical assistance. We also acknowledge Lea di Cioccio, Thierry Billon, and Catherine Pudda (CEA-LETI, Grenoble) for providing high-quality β-SiC(100) samples and E. Vlieg for the use of his wonderful ROD program. One of us, V. Yu. A., wishes to thank the RFBR for Grant No. 02-02-16811.

---

*On leave from Russian Academy of Sciences, Chernogolovka, Moscow District, Russia.

[1] *Silicon Carbide, A Review of Fundamental Questions and Applications to Current Device Technology*, edited by W. J. Choyke, H. M. Matsunami, and G. Pensl (Akademie, Berlin, 1998), Vols. I and II.

[2] *Properties of Silicon Carbide*, edited by G. Harris, EMIS Datareview Series (INSPEC, London, 1995), Vol. 13, and references therein.

[3] *Silicon Carbide Electronic Devices and Materials*, Special Issue on SiC of the Materials Research Society Bulletin, Vol. 22, March (1997); and references therein.

[4] V. M. Bermudez, Phys. Status Solidi B **202**, 447 (1997), and references therein.

[5] P. Soukiassian, Mater. Sci. Eng., B **61**, 506 (1999), and references therein.

[6] F. Bozso, L. Muehlhoff, M. Trenary, W. J. Choyke, and J. T. Yates, Jr., J. Vac. Sci. Technol. A **2**, 1271 (1984), and references therein.

[7] J. Bouix, M. P. Berthet, F. Bosselet, R. Favre, M. Peronnet, J. C. Viala, C. Vincent, and H. Vincent, J. Phys. IV **7**, 191 (1997), and references therein.

[8] J. C. Bokros, R. J. Akins, H. S. Shim, A. D. Hanbold, and N. K. Agarwal, CHEMTECH **7**, 40 (1977).

[9] K. L. Smith and K. M. Black, J. Vac. Sci. Technol. A **2**, 744 (1984).

[10] C. B. Duke, Chem. Rev. (Washington, D.C.) **96**, 1237 (1996).

[11] J. A. Kubby and J. J. Boland, Surf. Sci. Rep. **26**, 63 (1996).

[12] F. Semond, L. Douillard, P. Soukiassian, D. Dunham, F. Amy, and S. Rivillon, Appl. Phys. Lett. **68**, 2144 (1996).

[13] F. Amy, P. Soukiassian, Y.-K. Hwu, and C. Brylinski, Appl. Phys. Lett. **75**, 3360 (1999).

[14] F. Amy, H. Enriquez, P. Soukiassian, P. F. Storino, Y. J. Chabal, A. J. Mayne, G. Dujardin, Y. K. Hwu, and C. Brylinski, Phys. Rev. Lett. **86**, 4342 (2001).

[15] V. Derycke, P. Soukiassian, F. Amy, Y. Chabal, M. D'angelo, H. Enriquez, and M. Silly, Nat. Mater. **2**, 253 (2003).

[16] M. Dayan, J. Vac. Sci. Technol. A **3**, 361 (1985).

[17] M. Dayan, J. Vac. Sci. Technol. A **4**, 38 (1986).

[18] T. Yoshinobu, I. Izumikawa, H. Mitsui, T. Fuyuki, and H. Matsunami, Appl. Phys. Lett. **59**, 2844 (1991).

[19] S. Hara, W. F. J. Slijkerman, J. F. van der Veen, I. Ohdomari, S. Misawa, E. Sakuma, and S. Yoshida, Surf. Sci. Lett. **231**, L196 (1990).

[20] S. Hara, S. Misawa, S. Yoshida, and Y. Aoyagi, Phys. Rev. B **50**, 4548 (1994).

[21] F. Semond, P. Soukiassian, A. Mayne, G. Dujardin, L. Douillard, and C. Jaussaud, Phys. Rev. Lett. **77**, 2013 (1996).

[22] H. W. Yeom, Y. C. Chao, S. Terada, S. Hara, S. Yoshida, and R. I. G. Uhrberg, Phys. Rev. B **56**, R15 525 (1997).

[23] M. Lübbe, K. Lindner, S. Sloboshanin, S. Tautz, J. Schafer, and D. R. T. Zahn, J. Vac. Sci. Technol. A **16**, 3471 (1998).

[24] H. W. Yeom, Y. C. Chao, I. Matsuda, S. Hara, S. Yoshida, and R. I. G. Uhrberg, Phys. Rev. B **58**, 10 540 (1998).

[25] H. Yan, A. P. Smith, and H. Jónsson, Surf. Sci. **330**, 265 (1995).

[26] L. Pizzagalli, A. Catellani, G. Galli, F. Gygi, and A. Baratoff, Phys. Rev. B **60**, R5129 (1999).

[27] W. Lu, P. Krüger, and J. Pollmann, Phys. Rev. B **60**, 2495 (1999).

[28] W. Lu, W. G. Schmidt, E. L. Briggs, and J. Bernholc, Phys. Rev. Lett. **85**, 4381 (2000).

[29] U. Rossow, K. Lindner, M. Lübbe, D. E. Aspnes, D. R. T. Zhan, J. Vac. Sci. Technol. B **16**, 2355 (1998).

[30] R. Feidenhans'l, Surf. Sci. Rep. **10**, 105 (1989).

[31] I. K. Robinson and D. J. Tweet, Rep. Prog. Phys. **55**, 599 (1992).

[32] G. Renaud, Surf. Sci. Rep. **32**, 1 (1998).

[33] P. Soukiassian, F. Semond, L. Douillard, A. Mayne, G. Dujardin, L. Pizzagalli, and C. Joachim, Phys. Rev. Lett. **78**, 907 (1997).

[34] A. Catellani, G. Galli, F. Gygi, and F. Pellacini, Phys. Rev. B **57**, 12 255 (1998).

[35] A. Tejeda, D. Dunham, F. J. Garcia de Abajo, J. Dennlinger, E. Rotenberg, E. Garcia-Michel, and P. Soukiassian (unpublished).